A DNA Polymerase β Mutator Mutant with Reduced Nucleotide Discrimination and Increased Protein Stability[†,‡]

Amit M. Shah,[▽] Danyal A. Conn,[§] Shu-Xia Li,[▽,||] Andrew Capaldi,[§] Joachim Jäger,[§] and Joann B. Sweasy*[,▽]

Departments of Therapeutic Radiology and Genetics, Yale University School of Medicine, New Haven, Connecticut 06520, and School of Biochemistry and Molecular Biology, University of Leeds, Leeds LS2 9JT, United Kingdom

Received April 13, 2001; Revised Manuscript Received June 7, 2001

ABSTRACT: DNA polymerase β (pol β) offers a simple system to examine the role of polymerase structure in the fidelity of DNA synthesis. In this study, the M282L variant of pol β (M282Lβ) was identified using an in vivo genetic screen. Met282, which does not contact the DNA template or the incoming deoxynucleoside triphosphate (dNTP) substrate, is located on α-helix N of pol β. This mutant enzyme demonstrates increased mutagenesis in both in vivo and in vitro assays. M282Lβ has a 7.5-fold higher mutation frequency than wild-type pol β; M282Lβ commits a variety of base substitution and frameshift errors. Transient-state kinetic methods were used to investigate the mechanism of intrinsic mutator activity of M282Lβ. Results show an 11-fold decrease in dNTP substrate discrimination at the level of ground-state binding. However, during the protein conformational change and/or phosphodiester bond formation, the nucleotide discrimination is improved. X-ray crystallography was utilized to gain insights into the structural basis of the decreased DNA synthesis fidelity. Most of the structural changes are localized to site 282 and the surrounding region in the C-terminal part of the 31-kDa domain. Repositioning of mostly hydrophobic amino acid residues in the core of the C-terminal portion generates a protein with enhanced stability. The combination of structural and equilibrium unfolding data suggests that the mechanism of nucleotide discrimination is possibly affected by the compacting of the hydrophobic core around residue Leu282. Subsequent movement of an adjacent surface residue, Arg283, produces a slight increase in volume of the pocket that may accommodate the incoming correct base pair. The structural changes of M282Lβ ultimately lead to an overall reduction in polymerase fidelity.

Proofreading-deficient DNA polymerases in eukaryotes insert an incorrect nucleotide to produce single base substitution errors at a rate of 10^{-3} to $>10^{-6}$ (*1*). More recently, several other DNA polymerases have been identified (*2*), which appear to have a low fidelity (10^{-2}−10^{-3}) in the presence of undamaged DNA (*3, 4*). The broad range in error rates displayed by DNA polymerases is significantly less than the error rates predicted by the energy differences of hydrogen bonding between correct and incorrect base pairs (*5*). This suggests the polymerase itself discriminates between the correct and incorrect base pairs. Genomic errors produced by DNA polymerases have been suggested to be a contributor to human disease (*6*). Therefore, it is important to understand the structure−function relationships that govern faithful DNA synthesis.

DNA polymerase β (pol β),[1] one of the smallest eukaryotic polymerases, plays a role in many biological processes. Deletion of the pol β gene produces embryonic lethality in mice, due to apoptosis of postmitotic neurons (*7, 8*). This indicates that pol β is necessary for neurodevelopment. It is well documented that pol β plays a major role in base excision repair (BER). This enzyme removes 5′-deoxyribose phosphate and fills a DNA gap in the BER pathway (*9, 10*). Pol β is also implicated in playing a role in nucleotide excision repair (*11, 12*). Evidence has also suggested a meiotic function for pol β. During meiosis, pol β localizes to the synaptonemal complex in the first prophase of meiosis (*13*).

Pol β provides a natural model to relate polymerase structure to fidelity of DNA synthesis. The lack of accessory proteins, its small size (39 kDa), and no proofreading or exonuclease activities provide an ideal system to examine accurate DNA synthesis. These properties have facilitated kinetic characterization of wild-type pol β (WTβ). Pre-steady-state kinetic studies of WTβ (*14*) have shown a similar minimal kinetic pathway (Scheme 1) for DNA polymerization as other polymerases (*15, 16*). First, pol β binds to the DNA substrate, followed by binding to the deoxynucleoside triphosphate (dNTP) substrate. After formation of the ternary

[†] This work is supported by Grant CA80830 from the National Cancer Institute to J.B.S. and by a Yorkshire Cancer Research Grant to J.J. A.M.S. was supported by NIH Postdoctoral Fellowship F32-CA83250.

[‡] The PDB code for M28Lβ is 1JN3.

* Correspondence should be addressed to this author at the Department of Therapeutic Radiology, Yale University School of Medicine, 333 Cedar St., PO Box 208240, New Haven, CT 06520. E-mail: Joann.Sweasy@Yale.edu. Phone: (203) 737-2626. Fax: (203) 785-6309.

[▽] Yale University School of Medicine.

[§] University of Leeds.

[||] Present address: Curagen Corp., New Haven, CT.

[1] Abbreviations: BER, base excision repair; pol β, DNA polymerase β; dNTP, deoxynucleoside triphosphate; M282Lβ, leucine-substituted mutant protein of DNA polymerase β at methionine residue 282; Y265Hβ, histidine-substituted mutant protein of DNA polymerase β at tyrosine residue 265; WTβ, wild-type protein of DNA polymerase β.

10.1021/bi010755y CCC: $20.00
Published on Web 08/25/2001

Scheme 1: Minimal Kinetic Pathway of DNA Polymerization[a]

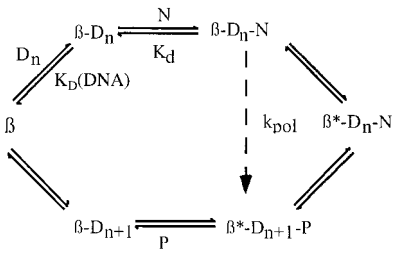

[a] β = DNA polymerase β, D = DNA, N = dNTP, and P= pyrophosphate.

complex of pol β, DNA, and dNTP, a conformational change occurs to produce an active complex (β*) that can catalyze DNA primer extension. After phosphodiester bond formation, pyrophosphate is released. Last, pol β dissociates from the DNA substrate. Mutator mutant proteins have been shown to alter kinetically the steps in the pathway of DNA polymerization (*17, 18*). This often leads to a decrease in fidelity.

Besides kinetic characterization, several high-resolution crystal structures have provided structural information of pol β (*19*−*25*). Despite having limited sequence homology and a different evolutionary history than other polymerases, the overall structure of the polymerase domain of WTβ shares a common architecture with other polymerases resembling a right hand (*26*−*28*). Determination of the crystal structures of mutator polymerases should identify possible structural changes that contribute to the reduction in fidelity.

To increase our understanding of polymerase structure−fidelity relationships, a genetic screen was used to identify mutator mutants of pol β (*29*). This genetic screen has been used to isolate several mutator mutants of pol β (*17, 18, 29, 30*). One of these mutants, Y265Hβ, shows a more than 100-fold loss in fidelity as compared to WTβ (*18*). The dramatic decrease in fidelity of this mutant enzyme is suggested to be an altered geometric alignment of catalytically important components, such as the position of the C-terminal domain relative to the active site residues and the DNA template. This leads to a very slow rate of polymerization for the correct dNTP substrate. In fact, the rate is only 8-fold faster than the incorrect nucleotide substrate. Another mutant, identified by the same genetic screen, is M282Lβ. Based on the crystal structure of pol β complexed with gapped-DNA and dNTP substrate (*24*), Met282 is located on α-helix N. This helix is repositioned upon binding of the incoming dNTP substrate, so that several amino acid residues can interact directly with the nascent base pair.

In this report, we describe the kinetic and structural characterization of the M282L mutator mutant of pol β. To determine the impact of amino acid residue Met282 on fidelity, the spontaneous mutation frequencies were determined in vivo and in vitro. A mutational spectrum of the mutant polymerase was also determined. This enzyme commits a variety of base substitution and frameshift errors. The biochemical basis of the mutator phenotype was investigated by using transient-state kinetic methods to compare the fidelity properties of M282Lβ to WTβ. The kinetic results show that M282Lβ has decreased fidelity. To gain insights into the structural basis of the reduced fidelity, the X-ray crystallographic structure of M282Lβ was solved to 2.35 Å. The structural results indicate that a tightening of the hydrophobic core around residue 282 is responsible for an overall improvement of the protein stability of the mutator mutant. A shift of residue Arg283 causes an increase in the volume of the DNA template·dNTP binding pocket. These changes may be reducing the fidelity properties of the mutant polymerase as compared to the wild-type protein. Thus, Met282 and the neighboring amino acid residues appear to play an important role in the mechanism of selecting the correct dNTP substrates over the incorrect ones.

MATERIALS AND METHODS

Bacterial Strains and Media. Escherichia coli B/r SC18-12 has the genotype *recA718polA12uvrA155trpE65 lon-11 sulA1*. This strain was used in the genetic screen for mutator mutants (*29*). *DH5*α with the genotype *mcrA* (*mrr-hsdRMS-mcrBC*) ϕ80Δ*lacZ*(M15 (*lacZYA-argF*)U169 *deoR recA1 endA1 phoA supE44 thi-1 gyrA96 relA1* was used in cloning experiments. BL21(DE3) with the genotype F$^-$*ompT hsdS*$_b$ (r_{b-} m_{b-}) *gal dcm* was used for protein expression. The FT334 strain with the genotype *recA13 upp tdk* was used in the forward mutation assay with the *Herpes simplex virus type 1* thymidine kinase (HSV-*tk*) as the mutational target (*31*). Media used are previously described (*17*).

Chemicals and Reagents. Deoxynucleoside triphosphates were purchased from New England BioLabs. Adenosine triphosphate (ATP) was purchased from Sigma. The [γ-^{32}P]-ATP (6000 μCi/μmol) was purchased from Amersham. Ultrapure grade urea was obtained from ICN Biomedicals Inc. Oligonucleotides were synthesized by Keck Molecular Biology Center at Yale University and purified by 20% acrylamide, 8 M urea polyacrylamide gel electrophoresis.

Detection of Mutator Mutants Using the Trp$^+$ Reversion Assay. A previously developed genetic screen (*29*) was used to identify M282Lβ. Briefly, mutator mutants were isolated using a Trp$^+$ reversion assay from a library of random pol β mutants. DNA from the pol β mutant library was used to transform the SC18-12 strain. Individual SC18-12 transformants were picked into Luria−Bertani broth (2 mL) containing 1 mM isopropyl β-D-thiogalactopyranoside (IPTG). Incubation was carried out at 37 °C for 16−24 h. Aliquots of cells were spread onto Eglu agar and incubated as described (*17, 29*). Mutants that produce Trp$^+$ revertants at significant frequencies over WTβ were isolated. The mutation of the M282Lβ gene was identified by DNA sequencing, which was performed by the Keck Molecular Biology Center at Yale University.

Expression and Purification of M282Lβ. The cDNA of M282Lβ was subcloned into the pET28a vector (Novagen) to generate a fusion protein containing six His residues attached to the amino terminus. Expression of M282Lβ in BL21(DE3) *E. coli* was induced with IPTG in Luria−Bertani broth containing kanamycin. The His-tagged protein was purified as previously described (*18*). Proteins were greater than 90% homogeneous based on a Coomassie blue-stained SDS−PAGE gel. The homogeneity and monodispersity of both M282Lβ and WTβ were assessed further by dynamic light scattering (DP-801, Protein Solutions Ltd). The purified protein was washed 3 times using a microconcentrator (Centriprep YM-10, Amicon) with an appropriate buffer [50 mM Tris-HCl, pH 8.0, for kinetics; 10 mM $(NH_4)_2SO_4$, 100

mM MES, pH 7.0, for crystallization; 150 mM KCl, 10 mM KH_2PO_4, pH 8.0, for urea-induced unfolding] and concentrated. Concentrations of pol β proteins were based on $\epsilon_{280} = 21\,200\ M^{-1}\ cm^{-1}$ and a molecular mass of 40 kDa for His-tagged pol β.

HSV-tk Forward Mutational Assay. To determine the intrinsic mutator activity of M282Lβ, purified pol β proteins were used to fill a 203-nucleotide gap, corresponding to the ATP binding site of the HSV-*tk* gene as described (*17*). Reactions contained 50 mM Tris-HCl (pH 8.0), 10 mM $MgCl_2$, 0.2 mM DTT, 0.2 g/L BSA, 500 μM dNTPs, 10 pmol of gapped DNA, and 100 pmol of WTβ or M282Lβ. Reactions were incubated for 1 h at 37 °C before being quenched with EDTA (30 mM = final concentration) and electroporated into FT334 cells. The spontaneous mutation frequency and the mutational spectrum were determined as described (*31*).

Single Base Pair Gapped DNA Preparation. A single base pair gapped DNA with a 5′-phosphate on the downstream oligonucleotide was used in all the experiments. The sequence of the DNA substrate is shown below:

45-22-22

5′-GCCTCGCAGCCGTCCAACCAAC CAACCTCGATCCAATGCCGTCC

3′-CGGAGCGTCGGCAGGTTGGTTGAGTTGGAGCTAGGTTACGGCAGG

The dNTP substrate was incorporated opposite template A (the position of the A is underlined). The primer oligomer was labeled at the 5′ end by using T4 polynucleotide kinase (New England BioLabs) and [γ-^{32}P]ATP. Other oligonucleotides were 5′-end-labeled with the kinase and normal ATP. Equimolar quantities of each DNA strand were annealed in 50 mM Tris-HCl, pH 8.0, containing 0.25 M NaCl. The mixture was incubated sequentially at 95 °C (5 min), slow-cooled to 50 °C (30 min), 50 °C (20 min), and immediately transferred to ice. To verify complete hybridization, the product was analyzed on an 18% native polyacrylamide gel followed by autoradiography.

Rapid Chemical Quench-Flow Experiments. A KinTek Instruments model RQF-3 rapid-quench-flow apparatus thermostated at 37 °C was used for rapid chemical quench-flow experiments as described (*18*). Reactions were performed in buffer [50 mM Tris-HCl buffer (pH 8.0) containing 2 mM DTT, 20 mM NaCl, and 10% glycerol]. All concentrations given refer to the final concentrations after mixing. Reactions were performed in which the pol β enzyme bound to DNA substrate was loaded in one loop and the dNTP substrate was loaded in the second loop. Reactions were initiated by rapid mixing of the pol β−DNA and Mg−dTTP solutions (final concentration of $MgCl_2$ = 10 mM). At selected time intervals, the reactions were quenched with 0.3 M EDTA.

To determine the K_d for dNTP and the maximum rate of polymerization (k_{pol}), incorporation of dTTP, dGTP, or dATP opposite template A was examined as a function of time. In these experiments, a solution containing a preincubated complex of WTβ or M282Lβ (500 nM) and gapped DNA (50 nM) was mixed with a solution of $MgCl_2$ (10 mM) and varying concentrations of a single dNTP. The enzyme to DNA ratio was determined by performing time courses at 5- and 10-fold enzyme concentration over gapped DNA substrate at 200 μM dTTP for M282Lβ. The different enzyme concentrations gave the same observed rate constant and amplitude. Thus, the rate of a single catalytic turnover of the enzyme is measured. Experiments for correct dNTP incorporation were performed on the KinTek rapid quench-flow apparatus, while experiments for misincorporation were performed manually as described (*18*). For each of the dNTP substrates, the reactions were performed under the same conditions.

Analysis of DNA binding affinity for gapped DNA by rapid chemical quench flow was essentially performed as described (*32*). Briefly, pol β (20 nM, determined by absorbance measurements) was preincubated with varying concentrations of radiolabeled gapped DNA. The pol β−DNA complex was then mixed with Mg−dTTP solution (10 mM Mg; 200 μM dTTP; final concentration) to start the reaction in the rapid quench-flow instrument. After 300 ms, the reaction was quenched. This time interval was selected based on previous pre-steady state burst experiments with wild-type pol β with gapped DNA substrate (*18*, *33*, *34*).

Products were resolved by sequencing gel electrophoresis under denaturing conditions (20% acrylamide containing 8 M urea) and quantified using a Molecular Dynamics Storm 840 Phosphorimager.

X-ray Crystallography. Crystals of the wild-type and mutant enzymes were grown at room temperature from hanging drops by mixing 2 μL of 13.5 mg/mL pol β (10 mM ammonium sulfate, 0.1 M MES, pH 7) with 2 μL of reservoir containing 13−20.0% PEG 3350, 50−300 mM sodium acetate, 50 mM HEPES, pH 7.5. Orthorhombic crystals of the 31-kDa domain with approximate dimensions of 150 × 150 × 150 μm appeared after 1 week. X-ray data were collected using a Rigaku RU200 rotating anode X-ray generator equipped with a Rigaku R-Axis IIC image plate system. Crystals of M282Lβ are isomorphous to the WTβ and belong to space group $P2_12_12_1$ (a = 119.6, b = 63.6, c = 37.6 Å). Data collection statistics are collated in Table 4.

Circular Dichroism Studies. Wild-type or mutant pol β protein (10 μM) in buffer (same buffer used in kinetic experiments) was incubated in a 0.2 cm path length quartz cuvette. The sample was then placed in a thermostated block in a circular dichroism spectrophotometer (Aviv model 62DS). Ellipticity was measured at 220 nm as a function of temperature over the range of 10−60 °C in 2.5 °C increments after the sample was equilibrated for 0.5 min at each temperature. Values were averaged for 15 s. The temperature at which the protein is 50% unfolded (T_m) was determined after the denaturation profile was subtracted by both upper and lower baselines. For the urea-induced protein denaturation, spectra were recorded on a JASCO J-715 circular dichroism spectrometer with a JASCO PTC-351S peltier element. Samples containing 0.2 g/L enzyme were prepared in 150 mM KCl, 10 mM KH_2PO_4, pH 8.0, with urea concentrations that varied in 0.1 M increments from 0.0 to 6.0 M. The samples were incubated overnight at 10 °C. Sweeping scans from 190 to 260 nm were carried out on the samples containing 0−6.0 M urea. The ellipticity at 225 nm was recorded 7 times for each sample, and the mean values were used to determine the free energy of unfolding, ΔG^{HOH}_{U-F}.

Data Analysis. Data obtained from kinetic assays were analyzed by using the KaleidaGraph program (Synergy

Table 1: Error Specificity by Class of M282Lβ and WTβ in the HSV-*tk* Forward Assay

	frequency $\times 10^{-4}$ (no. observed)		
	WTβ[a]	M282Lβ	M282Lβ/WTβ
MF_{obs}[b]	9.6 (68)	72.5 (68)	7.5
single	9.0 (64)	72.5 (0)	8.0
multiple	0.7 (4)	0 (0)	
base substitution	3.2	18.0	5.6
frameshift[c]	4.8	45.8	9.5

[a] Data taken from ref (*17*). [b] MF_{obs} is the average observed mutation frequency from at least three independent determinations. [c] Frameshifts include 1-base deletions or insertions.

Software). The kinetic parameters determined are shown in Scheme 1. Data from active site titrations were fit to the quadratic equation (*16*): $[E-DNA] = 0.5(K_{D(DNA)} + [E]_o + [D]_o) - [0.25(K_{D(DNA)} + [E]_o + [D]_o)^2 - ([E]_o[D]_o)]^{0.5}$, where [E−DNA] is the concentration of the pol β−DNA complex, $[E]_o$ is the initial enzyme concentration, $[D]_o$ is the initial concentration of the gapped DNA substrate, and $K_{D(DNA)}$ is the dissociation constant of the pol β−DNA complex. Single-turnover kinetic data were fit to the single-exponential equation: $[product] = A[1 - \exp(-k_{obs}t)]$, where A is the amplitude, t is the time, and k_{obs} is the observed rate constant. Observed rate constants were then plotted against [dNTP], and the data were fit to the hyperbolic equation: $k_{obs} = k_{pol}[dNTP]/(K_d + [dNTP])$, where k_{pol} is the maximum rate of polymerization and K_d is the equilibrium dissociation constant for dNTP. Fidelity values were calculated using the relationship: fidelity $= [(k_{pol}/K_d)_c + (k_{pol}/K_d)_i]/[(k_{pol}/K_d)_i]$, where c and i represent the correct and incorrect dNTPs, respectively.

RESULTS

M282Lβ Shows Mutator Activity in Vivo and in Vitro. To identify potential amino acid residues of pol β that are critical for fidelity, we used a genetic screen (*29*). One of the mutants we identified contains a Leu instead of a Met at amino acid residue 282. The spontaneous mutation frequency of M282Lβ in the *E. coli* Trp^+ reversion assay (*29*) is 13 times greater than WTβ.

M282Lβ Is a General Mutator Polymerase. To confirm the intrinsic mutator activity of M282Lβ, we used a forward mutation assay to determine the in vitro spontaneous mutation frequencies of wild-type and mutant pol β proteins (*31*). In this assay, WTβ or M282Lβ fills a 203-nucleotide gap of the HSV-*tk* gene at the ATP binding site. Errors committed by the polymerase during DNA synthesis can inactivate the HSV-*tk* gene. The inactive HSV-*tk* products are resistant to 5′-fluoro-2′-deoxyuridine.

In this assay, the spontaneous mutation frequencies for WTβ and M282Lβ were 9.6×10^{-4} and 72.5×10^{-4}, respectively, as shown in Table 1. Therefore, M282Lβ has a 7.5-fold higher spontaneous mutation frequency than WTβ. Thus, the mutant pol β protein shows a higher frequency for both in vivo and in vitro spontaneous mutations.

We characterized the frequency and types of mutations produced by M282Lβ using the HSV-*tk* forward mutation assay (*31*). We sequenced 68 *tk* mutants generated by M282Lβ in this assay, and compared them to the mutants produced by WTβ in the same assay (*17*). The mutation spectrum of M282Lβ is shown in Figure 1. A summary of the spectra of WTβ (*17*) and M282Lβ is presented in Table 1. The M282Lβ mutant produces both single-base substitution errors and 1-base frameshifts 5.6 and 9.5 times, respectively, more frequently than WTβ. Neither M282Lβ nor WTβ produces significant numbers of multiple mutations.

Few base substitution mutations were observed for either M282Lβ or WTβ (*17*). Neither polymerase produces T > A, T > G, G > C, C > A, or C > G base substitutions. M282L produces A > T mutations, followed by C > T, followed by A > G, G > T, and G > A at frequencies of 64 $\times 10^{-5}$, 31.9 $\times 10^{-5}$, and 21.3 $\times 10^{-5}$, respectively. WTβ produces G > T mutations, followed by A > T, followed by C > T at frequencies of 11.3 $\times 10^{-5}$, 10 $\times 10^{-5}$, and 8.5 $\times 10^{-5}$, respectively. Therefore, each of these polymerases appears to produce similar types of mutations among the most often observed ones.

Both M282Lβ and WTβ produce predominantly 1-base frameshift mutations. These frameshifts, which are mainly 1-base deletions, occur at several of the same positions within the *tk* target sequence. However, WTβ produced seven deletions of 1 base at position 250 of this target, whereas no 1-base deletions were observed at this position for M282Lβ. In addition, M282Lβ commited six 1-base deletion errors and one 1-base insertion at position 212, whereas WTβ does not have any mutations at this site, but instead commits predominantly 2-base deletions at position 214 of the *tk* gene. Another difference between these polymerases is that M282Lβ produced six 1-base insertions at position 142 and no 1-base frameshifts were observed for WTβ at this site. For both polymerases, most of the frameshift mutations occur at homonucleotide runs. In general, the error rate of 1-base frameshifts increased as a function of the length of the run, as shown in Table 2. However, no deletions were detected within a run of three nucleotides for WTβ, but nine frameshifts were observed at these sites for M282Lβ. Most of these frameshifts occurred at position 212, which is a run of three T residues. M282L is also able to commit frameshift errors within runs of three C residues. These data indicate that misalignment is the mechanism underlying the generation of many of the frameshift mutations observed in these spectra. In addition, all of these data suggest that M282Lβ is a general mutator polymerase, because it produces many types of base substitutions and a variety of frameshift mutations.

M282Lβ Has Reduced Discrimination of dNTPs. To understand the role of Met282 in DNA synthesis fidelity, we determined the ability of M282Lβ to incorporate dGTP and dATP substrates opposite adenine using a single base pair gapped DNA substrate. We chose to study the incorporation of dATP opposite template A because this was among the top three types of base substitution mutations produced by M282Lβ. We also characterized incorporation of dGTP opposite template A. A 10-fold excess of enzyme over the DNA substrate limits the pol β enzyme to a single-turnover of dNTP incorporation. This approach measures the ground-state binding of the dNTP, K_d, and the maximum rate of polymerization, k_{pol} (*18, 32*).

The K_d and k_{pol} values were determined by measuring the rate of product formation at varying concentrations of dNTP. Figure 2A shows the incorporation of dTTP opposite A for M282Lβ at several nucleotide concentrations. By fitting each

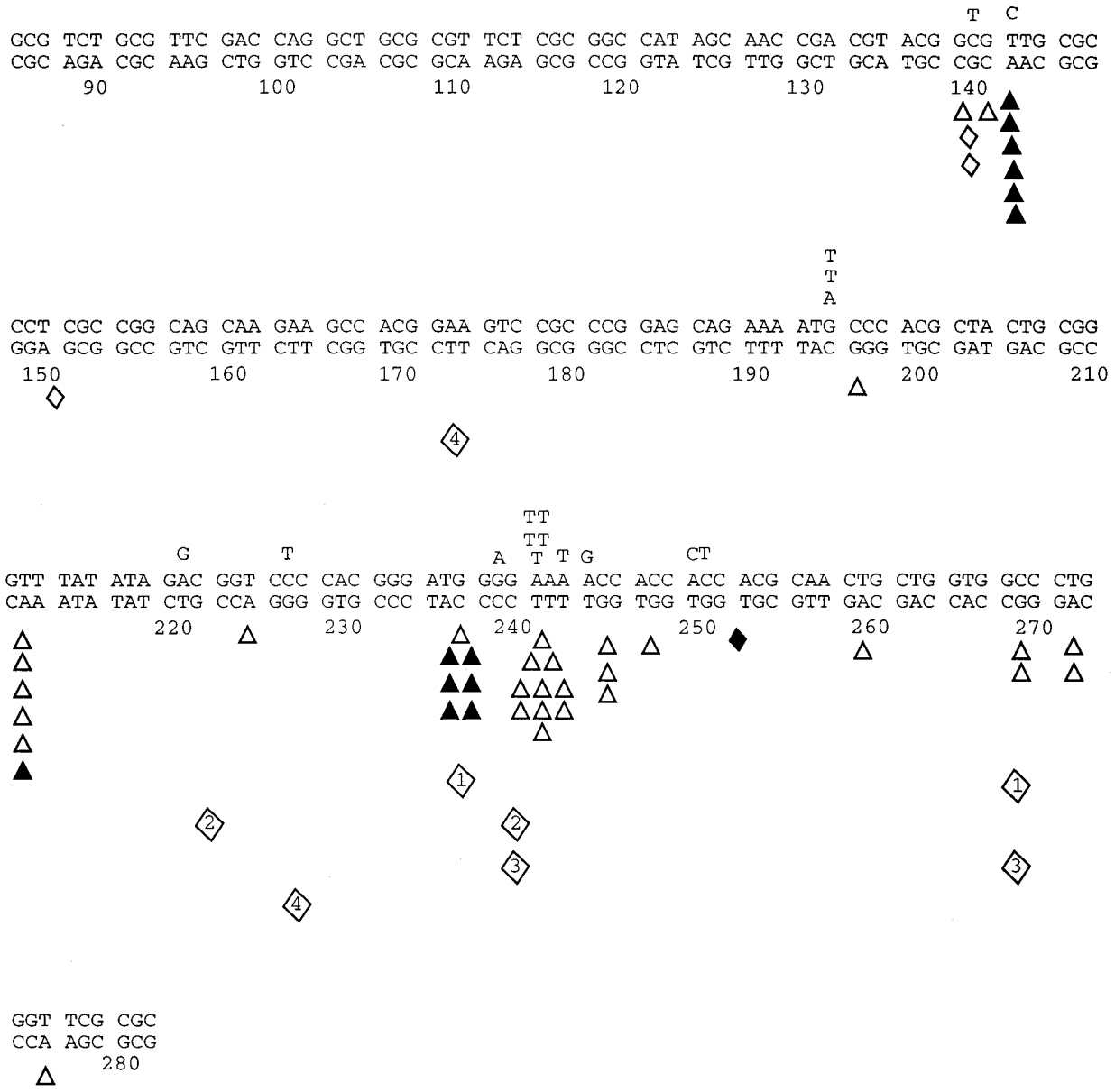

FIGURE 1: Mutational spectrum of M282Lβ. Mutations committed by M282Lβ as detected using the HSV-*tk* gap-filling assay. Frameshift errors, including 1-base insertions (▲), 1-base deletions (△), 2-base deletions (◇), 2-base insertions (◆), and large deletions (◇ with numbers inside), are shown under the HSV-*tk* target sequence. Base substitution mutations are shown above the target sequence.

Table 2: Frameshifts Generated by WTβ and M282Lβ at Different Lengths of Homonucleotide Runs

length of runs (bp)	error rate[a] × 10^{-5} (no. of mutants)		
	WTβ[b]	M282Lβ	M282Lβ/WTβ
1	0.048 (4)	0.260 (5)	5.4
2	0.52 (10)	5.20 (12)	10.0
3	<0.18 (0)	12.7 (9)	>70.5
4	7.1 (20)	45.2 (17)	6.4
error frequency	48 (34)	458 (43)	9.5

[a] Error rates were calculated by multiplying the total frameshift error frequency by the proportion of 1-base frameshifts at each repeat length per total frameshift and then dividing by the number of occurrences of each repeat length in the target sequence. [b] Data were taken from ref (*17*).

time course to the single-exponential rate equation, the k_{obs} was determined for each substrate concentration. These values were plotted against the dTTP concentrations to give the K_d and k_{pol} parameters for M282Lβ (Figure 2B). The values for K_d and k_{pol} are listed in Table 3 for incorporation of dTTP and misincorporation of dGTP and dATP opposite template A for both pol β enzymes.

The k_{pol} and K_d rate constants were used to calculate the fidelities for WTβ and M282Lβ. A 3-fold loss in fidelity was observed for M282Lβ ($F = 14\,100$) relative to WTβ ($F = 46\,900$) for G opposite template A. For A misincorporation opposite template A, the fidelity loss was minimal (3200 and 2300 for WTβ and M282Lβ, respectively). However, in both cases, the mechanism of discrimination is altered. The loss in fidelity reflects a reduced ability to discriminate between the correct versus the incorrect dNTP substrates at the level of ground-state binding (K_d) and a slightly enhanced ability to discriminate nucleotides at the k_{pol} level. For WTβ, the ground-state binding of the correct dNTP is 53 times stronger than the incorrect one, whereas M282Lβ displays a 5-fold difference between dTTP and dGTP and virtually no difference for dTTP and dATP. Thus,

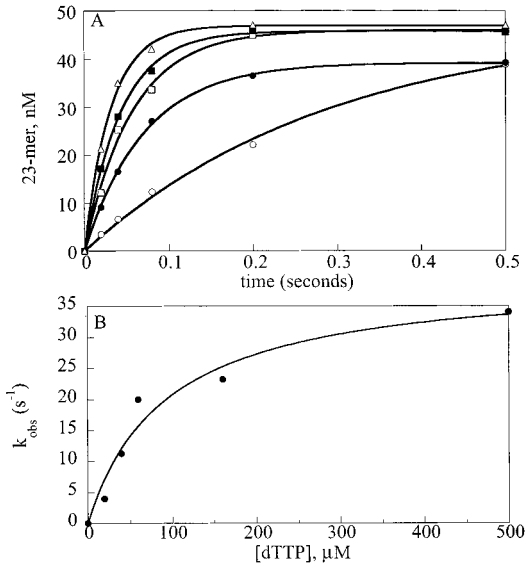

FIGURE 2: Single-turnover kinetic experiments of correct nucleotide incorporation opposite adenine. (A) Incorporation of dTTP opposite A for M282Lβ at 37 °C. A preincubated solution containing enzyme (500 nM) and gapped DNA (50 nM) was mixed with $MgCl_2$ (10 mM) and 20 (○), 40 (●), 60 (□), 160 (■), or 500 (△) μM dTTP. The reactions were quenched and monitored as described under Materials and Methods. Data were fit to the single-exponential equation to obtain k_{obs}. (B) Secondary kinetic plot of k_{obs} against dTTP concentration for M282Lβ (●). The data were fit to a hyperbolic equation as described under Materials and Methods. The solid line represents the best fit of the data to the hyperbolic equation. Values of K_d and k_{pol} are listed in Table 3.

substitution of Leu for Met-282 causes a 9- (7/0.8) to 11-fold (53/5) loss in discrimination at the level of K_d. However, the fidelity of M282Lβ appears to have slightly increased at the k_{pol} level. At this step, M282Lβ incorporates the correct nucleotide 2880−3035 times faster than the incorrect one, while WTβ shows a 860-fold difference. Thus, the mutant protein shows a 3−6-fold increase in discrimination at the level of k_{pol}. Therefore, M282Lβ has a reduced ability to discriminate at the level of K_d, which is compensated in part by an improved ability to distinguish correct dNTP substrates over incorrect ones at the k_{pol} level. Overall, this results in a pol β protein with lowered fidelity relative to wild-type pol β.

M282Lβ and WTβ Have Similar Binding for Gapped DNA. Active-site titrations were conducted to measure the $K_{D(DNA)}$ for formation of a productive complex between the gapped DNA substrate and M282Lβ or WTβ. The titration was performed by preincubating a fixed concentration of pol β protein with increasing concentrations of the gapped DNA substrate. This mixture was then reacted for 0.3 s with the correct dNTP substrate, dTTP. The selected time interval allowed adequate time to reach maximum amplitude with minimal contribution of multiple catalytic turnovers. Thus, this method also provides a measurement of the amount of active E−DNA complex present.

The DNA dependence of the amplitude is shown in Figure 3 for M282Lβ and WTβ. The $K_{D(DNA)}$ value for an active complex between the mutant protein and gapped DNA was 112 ± 5 nM with a maximum amplitude of 8 ± 0.1 nM. The $K_{D(DNA}$ and maximum amplitude for wild-type pol β were 70 ± 11 nM and 6 ± 0.4 nM, respectively. The $K_{D(DNA)}$ value for WTβ was similar to a previous measurement performed with duplex DNA (*14*). Dissociation constants of pol β−gapped DNA complex for the two proteins showed a less than 2-fold difference, suggesting that the Leu substitution at amino acid residue 282 does not significantly impact on the binding of pol β to a gapped DNA substrate.

M282Lβ Structural Changes Are Confined to Residue 282 and Neighboring Amino Acid Residues. To gain insights into the structural basis of the fidelity of M282Lβ, we tried to crystallize the apoenzyme and the enzyme in the presence of DNA and dNTP substrates. Only the apoenzyme yielded crystals. The X-ray crystal structure of the mutator polymerase apoenzyme was determined (Figure 4). A difference density map with coefficients $F^{wt}_{obs} - F^{mut}_{obs}$ was calculated using phases from a rigid body refined model of M282Lβ. The only noticeable difference density of 3σ above the mean is located in the C-terminal part of the 31-kDa domain and essentially corresponds to the Sδ and Cϵ atoms of Met282 in the wild-type protein, which is absent from M282Lβ.

Both WTβ and M282Lβ structures have been refined to *R*-values of 0.256 and 0.257, respectively (Table 4). The overall structures essentially remain unchanged for both proteins as seen from the refined crystal structures (Figure 5). The Cα atom positions in the two models can be superimposed with an overall rms of 0.3 Å. Most of the structural differences observed in the mutant protein are confined to loops not involved in crystal contacts. These regions typically display temperature factors above 70 Å^2.

There is a concerted shift of amino acid side chains in the C-terminal domain on the DNA binding surface near residue 282. The side chains of Arg283, Leu287, Ile293, and Glu295 have changed position by up to 0.9 Å in order to maintain the proximity to Leu282. Furthermore, backbone atoms positions of Asn294 and Glu295 in the lower part of the β-strand (residues Phe291−Asn294, β-sheet 3) appear to have moved toward α-helix N (residues Asp276−Glu288) when compared with the WTβ structure.

Alterations in the hydrogen-bonding network around residue 282 can be observed by comparing the wild-type and mutant protein structures. Hydrogen bonds are present in WTβ between Ser275 N and Asn279 Nδ2, but are missing in M282Lβ. Conversely, hydrogen bonds between Lys289 Nη and Gln324 Oϵ1, and between Thr292 O and Arg299 Nη1, appear in M282Lβ, but not in WTβ.

Overall, these structural differences suggest a change in stability in M282Lβ, which prompted us to investigate the differences in protein stability between M282Lβ and WTβ.

M282Lβ Is a More Stable Protein than WTβ. We have used circular dichroism spectroscopy to determine the α-helical content of both M282Lβ and WTβ as a function of temperature and urea. The T_m values are 42 °C for WTβ and 48 °C for M282Lβ (Figure 6), suggesting that the amino acid alteration stabilizes the pol β mutant protein. To verify the observed protein stability for M282Lβ, circular dichroism spectra were collected in the presence of the chemical denaturant urea. Protein denaturation by urea gave rise to the equilibrium unfolding curves for WTβ and M282Lβ shown in Figure 7. The values of ΔG^{HOH}_{U-F} obtained for M282Lβ and WTβ are 7.1 ± 1.1 and 22.9 ± 0.9 kJ/mol, respectively. Thus, the free energy of unfolding for the mutant protein is lower than wild-type protein, indicating

Table 3: Single-Turnover Kinetic Values for WTβ and M282Lβ

	k_{pol} (s^{-1})	K_d (μM)	$k_{pol(c)}/k_{pol(i)}$[e]	$K_{d(i)}/K_{d(c)}$[f]	k_{pol}/K_d (M^{-1} s^{-1})	F ($\times 10^3$)[g]
WTβ[a]						
A:T[b]	9.7 ± 0.7	11 ± 2			8.82×10^5	
A:G[c]	0.0113 ± 0.0007	601 ± 96	860	53	18.8	46.9
A:A[d]	0.0201 ± 0.0018	75 ± 21	480	7	268	3.2
M282Lβ						
A:T	39.8 ± 4.6	92 ± 28			4.33×10^5	
A:G	0.0138 ± 0.0007	451 ± 67	2880	5	30.6	14.1
A:A	0.0131 ± 0.0022	69 ± 20	3035	0.8	190	2.3

[a] Values for WTβ are from ref (*18*). [b] Kinetic parameters for incorporation of dTTP opposite template A. [c] Kinetic values for misincorporation of dGTP opposite template A. [d] Kinetic values for misincorporation of dATP opposite template A. [e] The k_{pol} for correct (c) divided by incorrect (i). [f] The K_d for incorrect (i) dNTP divided by correct (c). [g] Fidelity (F) was calculated as described under Materials and Methods.

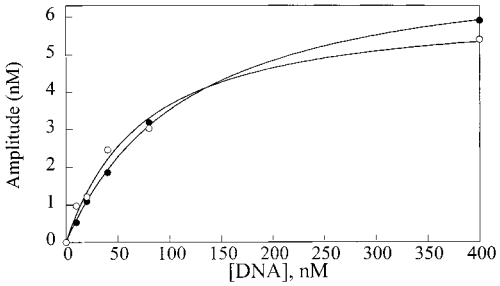

FIGURE 3: DNA binding by titration of enzyme active sites. WTβ (○) or M282Lβ (●) (20 nM, determined by absorbance measurements) was preincubated with increasing concentrations of radiolabeled gapped DNA. The pol β−DNA complex was then mixed with Mg−dTTP solution to initiate the reaction in the rapid quench-flow apparatus. The reaction was quenched after 300 ms and quantitated as described under Materials and Methods. The $K_{D(DNA)}$ values for an active complex between the mutant protein and gapped DNA were 112 ± 5 and 70 ± 11 nM for wild-type pol β.

that overall the substitution of Met282 to Leu has a stabilizing effect on the pol β structure.

DISCUSSION

A genetic screen was used to detect a DNA polymerase β mutant protein, which coded for Leu at position 282 instead of Met. This screen was developed to identify mutator mutants of DNA polymerase β (*29*). In this study, we demonstrate intrinsic mutator activity for M282Lβ. The molecular basis for the mutator activity appears to be a loss in dNTP discrimination at the level of ground-state binding,

Table 4: Summary of Data Collection and Structure Refinement Statistics

pol β	WT	M282L
unit cell dimensions (a, b, c) (Å)	119.4, 63.46, 37.08	119.6, 63.60, 37.56
resolution (Å)	2.60	2.35
rotation per frame (deg)	2.0	2.0
detector to crystal distance (cm)	148.6	140.4
total no. of reflections	53992	89772
no. of unique reflections	8364	11677
completeness (last shell) (%)	91.6 (71.4)	93.4 (65.3)
R_{sym}[a] (last shell) (%)	8.1 (23.2)	8.0 (24.4)
overall B	31.38	28.17
R-value (free)	0.257	0.256
rms (bond) (Å)	0.007	0.009
rms (angle) (deg)	1.345	1.503
rms (dihedral) (deg)	23.414	23.716

[a]
$$R_{sym} = \frac{[\sum_{-hkl}^{hkl}\sum_{j=1}^{N} I_j^{hkl} - \langle I_{hkl}\rangle]}{[\sum_{-hkl}^{hkl}\sum_{j=1}^{N} I_j^{hkl}]}$$

K_d. The reduced discrimination experienced at this step of the kinetic pathway is partially compensated by an improved ability to discriminate dNTP substrates at the k_{pol} level. The difference in the mechanism of nucleotide discrimination is suggested to result from subtle structural changes localized around amino acid residue 282 of pol β. Thus, Met282, which

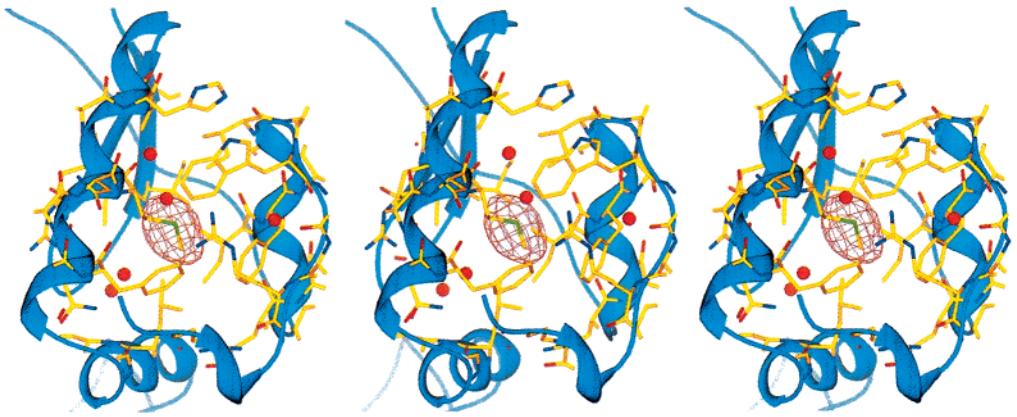

FIGURE 4: X-ray crystallographic structure of M282Lβ. A stereo diagram showing a ribbon drawing of the C-terminal domain of M282Lβ (cyan) superimposed on the $F_o^{wt} - F_o^{mut}$ difference electron density map (red) contoured at 3.3σ above the mean density of the asymmetric unit. Leu282 and neighboring residues from mutant structure are shown in atom colors. The stereo diagram was generated using the program SPOCK.

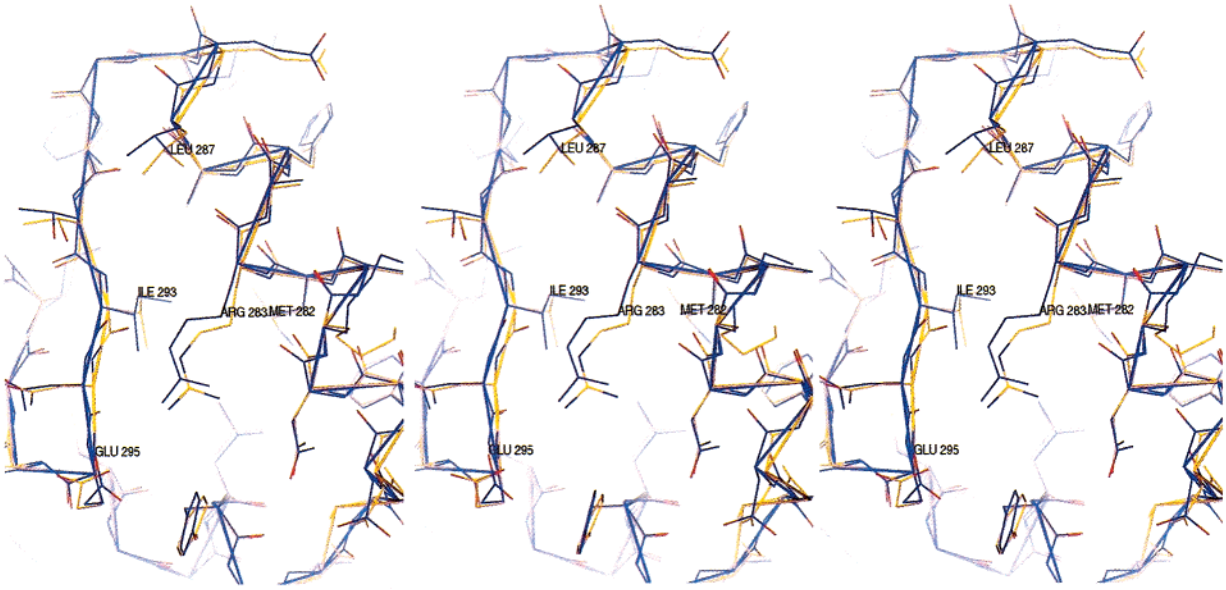

FIGURE 5: Comparison of the α-carbon traces of the mutator polymerase (blue) and the wild-type protein (cyan). Only the coordinates of α-carbon atoms within the C-terminal domains were used to superimpose the structures of WTβ (cyan) and M282Lβ (blue). The side chain atoms of residues Arg283, Leu287, Leu293, Asn294, Glu295, and Met- or Leu282 are shown to highlight the differences in packing around the site of mutation. Please note that residues Arg283 and Ile293 move between 0.6 and 0.9 Å closer to the core of the C-terminal domain. These changes along with a shortening of several crucial hydrogen bonds lead to an increase in overall protein stability for M282Lβ. The stereo diagram was generated using the program SPOCK.

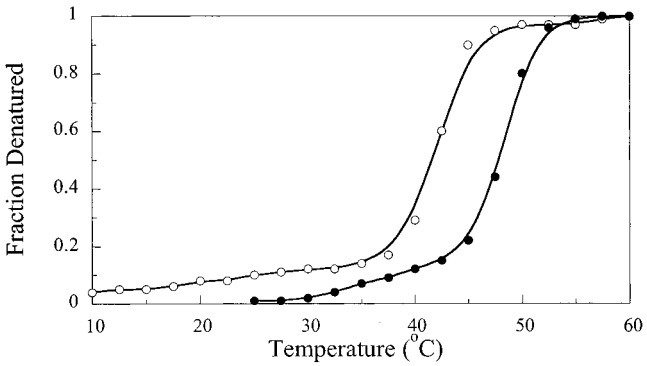

FIGURE 6: Heat denaturation of pol β proteins. A solution of WTβ (○) and M282Lβ (●) was placed in a thermostated block in a CD spectrophotometer as described under Materials and Methods. Ellipticity was measured at 220 nm as a function of temperature over the range of 10−60 °C. The fraction denatured was determined, and the temperature at which the protein is 50% unfolded was determined by interpolation.

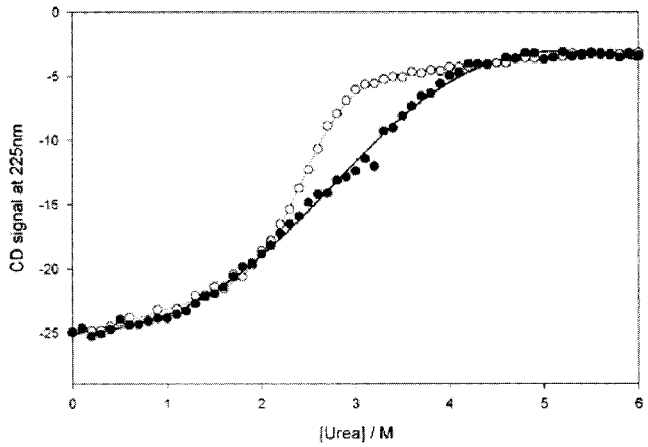

FIGURE 7: Urea-induced unfolding of pol β. Graph showing equilibrium unfolding curves fitted by nonlinear regression for WTβ (○) and M282Lβ (●) at 225 nm, 10 °C, in the presence of increasing concentrations of urea as described under Materials and Methods.

is absent of any direct contact with Mg ions, template, primer, or the incoming dNTP, is critical for fidelity of pol β and contributes to dNTP discrimination at the level of ground-state binding.

M282Lβ Is a Mutator Polymerase. The polymerase activity of M282Lβ displays characteristics of a mutator phenotype. In general, a polymerase that incorporates mutations more frequently than a normal enzyme is defined as a mutator. Mutator phenotypes have been suggested to be one of the underlying causes of cancer at the molecular level (*35*). Many lines of evidence are consistent with the interpretation of M282Lβ as a mutator polymerase. First, the M282Lβ mutant is able to revert at a high frequency the *trpE65* chromosomal mutation in the SC18-12 *E. coli* strain. To accomplish the Trp reversion, M282Lβ mutant needs to insert a mutation to produce a base substitution error within the *trpE* gene or a supressor tRNA. Second, the mutant protein has an increased spontaneous mutation frequency relative to wild-type pol β in the HSV-*tk* forward mutation assay. Third, the mutation spectrum of M282Lβ indicates that the mutant polymerase commits base substitution and frameshift errors more frequently than WTβ. Thus, both in vivo and in vitro assays confirm a mutator phenotype for M282Lβ.

The results of the single-turnover kinetic experiments show a lower fidelity for misincorporation opposite template A with a single-base-pair gapped DNA substrate. The modest decrease in fidelity is a result of M282Lβ undergoing contrasting abilities of dNTP substrate discrimination at different steps in the kinetic pathway. At the level of ground-state binding of dNTP, M282Lβ shows an 11-fold (53/5) decrease relative to WTβ in distinguishing between dGTP and dTTP and a 9-fold (7/0.8) reduction in discriminating between dATP and dTTP. This result should predict a larger

decrease in fidelity. However, there is also a 3−6-fold enhanced discrimination at the level of k_{pol}, the maximum rate of polymerization, for the mutant protein. This value encompasses two steps in the kinetic pathway: the conformational change and nucleotidyl transfer. Thus, the ability to incorporate dNTP substrates accurately appears to be improved at least at one of these two steps for M282Lβ. Consequently, the discrimination loss at the level of ground-state binding is compensated by the improved ability to select the correct dNTP substrate over the incorrect ones at the level of k_{pol}.

Subtle Changes in van der Waals Interactions and Hydrogen Bonding Increase M282Lβ Stability. The structural differences between M282Lβ and WTβ are restricted to the site of mutation and the surrounding residues (Figure 5). The structures of the N-terminal and central parts of the 31-kDa domain remain unchanged. The crystal structures of the two pol β proteins show subtle differences in the hydrogen-bonding network within the C-terminal portion of 31-kDa domain. In a direct comparison, the majority of hydrogen bonds in M282Lβ appear to be shorter than those formed in WTβ. Denaturation experiments of the two proteins show that M282Lβ unfolds less readily than WTβ. Thus, the increase in van der Waals interactions, the apparent tightening of the hydrophobic core, and a strengthening of the hydrogen-bonding network in M282Lβ seem to lead to a more stable protein for the mutant polymerase.

In the structure of WTβ complexed with gapped DNA duplex, Arg283 directly contacts the minor groove edge of the templating nucleotide (*23*, *24*, *36*). Met282 interacts with the aliphatic side chain of Arg283 and, thus, has a stabilizing effect by reducing the flexibility of the Arg side chain. An arginine to alanine substitution at position 283 has a large impact on fidelity (*37*, *38*), mainly due to a large decrease at the level of k_{pol}. In M282Lβ, the amino acid substitution enhances discrimination at the k_{pol} level. This implies that amino acid residue 282, which is not in direct contact with the DNA template, does not substantially contribute to nucleotide discrimination at the level of k_{pol}. However, the reduction in side chain volume from Met282 to Leu in M282Lβ is propagated to the position of Arg283, which in turn may favor a re-alignment of the DNA template, the 3′OH of the primer, and the incoming nucleotide in such a way that the pol β mutant enzyme reduces nucleotide selectivity at the level of ground-state dNTP binding. Thus, amino acid residue 282 has an indirect effect on the mechanism of dNTP substrate discrimination.

Conclusion. In summary, M282Lβ was identified by an in vivo genetic screen that detects mutator polymerases. This enzyme demonstrates elevated mutagenesis in both in vivo and in vitro assays. Transient-state kinetic results show a significant decrease in dNTP substrate discrimination at the level of ground-state binding by 9−11-fold. During the protein conformational change and/or the nucleotidyl transfer steps, the discrimination of dNTP substrates is slightly improved. The crystallographic structure of the mutant polymerase shows that subtle structural changes around Leu282 lead to a tightening of the hydrophobic core in the C-terminal part of the 31-kDa domain, resulting in a more stable protein as assessed by temperature and urea-induced unfolding. Overall, M282Lβ has reduced DNA synthesis fidelity.

REFERENCES

1. Kunkel, T. A., and Bebenek, K. (2000) *Annu. Rev. Biochem. 69*, 497−529.
2. Friedberg, E. C., Feaver, W. J., and Gerlach, V. L. (2000) *Proc. Natl. Acad. Sci. U.S.A. 97*, 5681−5683.
3. Matsuda, T., Bebenek, K., Masutani, C., Hanaoka, F., and Kunkel, T. A. (2000) *Nature 404*, 1011−1013.
4. Johnson, R. E., Washington, T., Prakash, S., and Prakash, L. (2000) *J. Biol. Chem. 275*, 7447−7450.
5. Loeb, L. A., and Kunkel, T. A. (1982) *Annu. Rev. Biochem. 51*, 429−457.
6. Loeb, L. A. (1998) *Adv. Cancer Res. 72*, 25−56.
7. Sobol, R. W., Horton, J. K., Kuhn, R., Gu, H., Singhal, R. K., Prasad, R., Rajewsky, K., and Wilson, S. H. (1996) *Nature 379*, 183−186.
8. Sugo, N., Aratani, Y., Nagashima, Y., Kubota, Y., and Koyama, H. (2000) *EMBO J. 19*, 1397−1404.
9. Matsumoto, Y., and Kim, K. (1995) *Science 269*, 699−702.
10. Wilson, S. H. (1998) *Mutat. Res. 407*, 203−215.
11. Horton, J. K., Srivastava, D. K., Zmudzka, B. Z., and Wilson, S. H. (1995) *Nucleic Acids Res. 23*, 3810−3815.
12. Oda, N., Saxena, J. K., Jenkins, T. M., Prasad, R., Wilson, S. H., and Ackerman, E. J. (1996) *J. Biol. Chem. 271*, 13816−13820.
13. Plug, A. W., Clairmont, C. A., Sapi, E., Ashley, T., and Sweasy, J. B. (1997) *Proc. Natl. Acad. Sci. U.S.A. 94*, 1327−1331.
14. Werneburg, B. G., Ahn, J., Zhong, X., Hondal, R. J., Kraynov, V. S., and Tsai, M. D. (1996) *Biochemistry 35*, 7041−7050.
15. Benkovic, S. J., and Cameron, C. E. (1995) *Methods Enzymol. 262*, 257−269.
16. Patel, S. S., Wong, I., and Johnson, K. A. (1991) *Biochemistry 30*, 511−525.
17. Li, S., Vaccaro, J., and Sweasy, J. B. (1999) *Biochemistry 38*, 4800−4808.
18. Shah, A. M., Li, S.-X., Anderson, K. S., and Sweasy, J. B. (2001) *J. Biol. Chem. 276*, 10824−10831.
19. Pelletier, H., Sawaya, M. R., Kumar, A., Wilson, S. H., and Kraut, J. (1994) *Science 264*, 1891−1903.
20. Pelletier, H., and Sawaya, M. R. (1996) *Biochemistry 35*, 12778−12787.
21. Pelletier, H., Sawaya, M. R., Wolfle, W., Wilson, S. H., and Kraut, J. (1996) *Biochemistry 35*, 12742−12761.
22. Pelletier, H., Sawaya, M. R., Wolfle, W., Wilson, S. H., and Kraut, J. (1996) *Biochemistry 35*, 12762−12777.
23. Sawaya, M. R., Pelletier, H., Kumar, A., Wilson, S. H., and Kraut, J. (1994) *Science 264*, 1930−1935.
24. Sawaya, M. R., Prasad, R., Wilson, S. H., Kraut, J., and Pelletier, H. (1997) *Biochemistry 36*, 11205−11215.
25. Arndt, J. W., Gong, W., Zhong, X., Showalter, A. K., Liu, J., Dunlap, C. A., Lin, Z., Paxson, C., Tsai, M.-D., and Chan, M. K. (2001) *Biochemistry 40*, 5368−5375.
26. Jäger, J., and Pata, J. D. (1999) *Curr. Opin. Struct. Biol. 9*, 21−28.
27. Joyce, C. M., and Steitz, T. A. (1995) *J. Bacteriol. 177*, 6321−6329.
28. Steitz, T. A. (1999) *J. Biol. Chem. 274*, 17395−17398.
29. Washington, S. L., Yoon, M. S., Chagovetz, A. M., Li, S., Clairmont, C. A., Preston, B. D., Eckert, K. A., and Sweasy, J. B. (1997) *Proc. Natl. Acad. Sci. U.S.A. 94*, 1321−1326.
30. Sweasy, J. B., Chen, M., and Loeb, L. A. (1995) *J. Bacteriol. 177*, 2923−2925.
31. Eckert, K. A., Hile, S. E., and Vargo, P. L. (1997) *Nucleic Acids Res. 25*, 1450−1457.
32. Kati, W. M., Johnson, K. A., Jerva, L. F., and Anderson, K. S. (1992) *J. Biol. Chem. 267*, 25988−25997.
33. Ahn, J. W., Kraynov, V. S., Zhong, X. J., Werneburg, B. G., and Tsai, M. D. (1998) *Biochem. J. 331*, 79−87.
34. Vande Berg, B. J., Beard, W. A., and Wilson, S. H. (2001) *J. Biol. Chem. 276*, 3408−3416.
35. Loeb, L. A., Springgate, C. F., and Battula, N. (1974) *Cancer Res. 34*, 2311−2321.
36. Osheroff, W. P., Beard, W. A., Wilson, S. H., and Kunkel, T. A. (1999) *J. Biol. Chem. 274*, 20749−20752.

37. Beard, W. A., Osheroff, W. P., Prasad, R., Sawaya, M. R., Jaju, M., Wood, T. G., Kraut, J., Kunkel, T. A., and Wilson, S. H. (1996) *J. Biol. Chem. 271*, 12141−12144.

38. Ahn, J., Werneburg, B. G., and Tsai, M. D. (1997) *Biochemistry 36*, 1100−1107.

BI010755Y